



Research paper

Pyrazoline derivatives of acryloyl substituted ferrocenyl ketones: Synthesis, antimicrobial activity and structural properties



Adrijana Burmudžija^a, Jovana Muškinja^a, Zoran Ratković^{a,*}, Marijana Kosanić^b, Branislav Ranković^b, Sladjana B. Novaković^c, Goran A. Bogdanović^c

^a Department of Chemistry, Faculty of Science, University of Kragujevac, Radoja Domanovića 12, 34000 Kragujevac, Serbia

^b Department of Biology and Ecology, Faculty of Science, University of Kragujevac, Radoja Domanovića 12, 34000 Kragujevac, Serbia

^c Vinča Institute of Nuclear Sciences, Laboratory of Theoretical Physics and Condensed Matter Physics, University of Belgrade, P.O. Box 522, 11001 Belgrade, Serbia

ARTICLE INFO

Article history:

Received 15 September 2017

Received in revised form 27 November 2017

Accepted 28 November 2017

Available online 2 December 2017

Keywords:

Ferrocenyl ketones
Enone system
Pyrazoline derivatives
Crystal structure
Antimicrobial activity

ABSTRACT

A series of ferrocenyl ketones were synthesized in reaction with ferrocene and corresponding substituted acryloyl chlorides, following previously described procedure. Synthesized products have conjugated enone system, which is suitable for further transformations. In a reaction with hydrazine in acidic medium (acetic acid) new pyrazoline derivatives were obtained. Their antimicrobial properties have been tested. Synthesized pyrazoline derivatives demonstrated expressed *in vitro* antimicrobial activity towards 12 strains of microorganisms inhibiting all tested bacteria and fungi. The most potent compound in all cases was sorbyl derivative; for bacteria activity was very close to streptomycin, and for fungi in one case the same as ketoconazole. It is established that this compound can be a new, potential antimicrobial agent with minimum inhibitory concentrations from 0.039 to 0.312 mg/mL. One of the starting compounds and two products were crystal substances, suitable for the single crystal X-ray diffraction analysis, which confirmed undoubtedly their structures.

© 2017 Elsevier B.V. All rights reserved.

1. Introduction

Chalcones (1,3-diaryl-2-propen-1-ones), and chalcone-like compounds (with similar enone system) are an important class of organic compounds, since they often represent core structure of many natural products and exhibit various pharmacological and biological activities. Antimicrobial [1–6], antioxidant [7–9], antifungal [5,6,10], antimalarial [11–13], anti-inflammatory [14,15] and anticancer activity [16–21] are well expressed and explored. Enone system presented in chalcones is the often a key part of substrates; it is almost planar and have *trans*-double bond. This structure enables various transformations of enone system, which could be easily converted into different heterocyclic derivatives, in reactions with urea, thiourea, hydroxylamine, hydrazine, guanidine [22,23], forming heterocyclic unit between aromates. Ferrocenyl derivatives are among the most promising organometallic compounds which can be used in microbiological research. In continuation of our interest in synthesis of ferrocene containing heterocycles exhibiting some biological activities [24–27], we expected that incorporation of pyrazoline fragment

and the ferrocene scaffold into the same molecule might have an attracting structural result for development of novel antimicrobial agents. Herein we wish to report on synthesis, spectral characterization and evaluation of antimicrobial activity on some strains of microorganisms a series of novel Fc-pyrazoline derivatives, prepared from chalcone-like ketones (**2a–e**) and heterocyclic chalcone **2f**. All new products were characterized by their spectral data (IR, MS, ¹H NMR and ¹³C NMR). Compounds **2c**, **3c** and **3f** gave crystals suitable for the X-ray analysis

2. Experimental

2.1. Chemistry

2.1.1. Materials and measurements

All starting chemicals were commercially available and used as received, except for the solvents being purified by distillation. Column chromatography were carried out using silica gel 60 (Merck, 230–400 mesh ASTM); for TLC was used Silica gel 60 F₂₅₄-pre-coated plates (Merck); layer thickness 0.2 mm. IR spectra: Perkin-Elmer Spectrum One FT-IR spectrometer with a KBr disc, ν in cm⁻¹. NMR spectra: Varian Gemini 200 MHz spectrometer (200 MHz for ¹H and 50 MHz for ¹³C), using CDCl₃ as the solvent and

* Corresponding author.

E-mail address: wor@kg.ac.rs (Z. Ratković).

TMS as the internal standard. ^1H and ^{13}C NMR chemical shifts were reported in parts per million (ppm) and were referenced to the solvent peak; CDCl_3 (7.26 ppm for ^1H and 76.90 ppm for ^{13}C). Multiplicities are represented by s (singlet), d (doublet), t (triplet), q (quartet) and m (multiplet). Coupling constants (J) are in Hertz (Hz). Mass spectrometry was performed by Waters Micromass ZQ mass spectrometer and MassLynx software for control and data processing. Electro spray ionization in the positive mode was used. The electro spray capillary was set at 4.3 kV and the cone at 40 V. The ion source temperature was set at 125 °C and the nitrogen flow rates were 400 L/h and 50 L/h, for desolvation and cone gas flow respectively. The collision energy was 40 eV. The melting point of products was determined by using MelTemp1000 apparatus.

2.1.2. Procedure for the synthesis of 1-ferrocenyl-2,4-hexadien-1-one (**2e**)

The ferrocenyl ketone, 1-ferrocenyl-2,4-hexadien-1-one (sorbic ferrocene), **2e**, was prepared by following procedure: sorbic acid, 1.12 g (10 mmol) was dissolved in a 150 mL of dried CH_2Cl_2 , and 1 mL of PCl_3 was added. Closed vessel with solution was stirred overnight at room temperature. To this solution 1.98 g of ferrocene (10 mmol) was added following with 1.44 g (10 mmol) of anhydrous AlCl_3 . Solution became deep blue from formed complex, and stirring was continued for next 2–3 h. Reaction mixture was poured out in 100 mL of 2 M HCl solution and shaken well. Organic phase was separated, and water layer was extracted with 50 mL of CH_2Cl_2 . Combined organic layers were washed with 2×100 mL of water and dried over anhydrous Na_2SO_4 . The main part of solvent was removed by distillation and concentrated crude mixture was filtered through SiO_2 pad. Separation of product was performed on SiO_2 column using CH_2Cl_2 as eluent. Deep red band belongs to ferrocenyl ketone **2e**. Solvent was evaporated by distillation and products crystallizes on standing.

Cinnabar red crystals; mp 139–140 °C; Yield 75%; IR (cm^{-1}): 3118, 3017, 1652, 1627, 1583, 1457, 1376, 1267, 1104, 1072, 1001; ^1H NMR: δ 1.89 (d, $J = 5.4$ Hz, 3H), 4.18 (s, 5H), 4.54 (t, $J = 2.2$ Hz, 2H), 4.83 (t, $J = 1.8$ Hz, 2H), 6.22–3.38 (m, 2H), 6.48 (d, $J = 15.4$ Hz, 1H), 7.27–7.44 (m, 1H); ^{13}C NMR: δ 18.8, 69.6, 70.0, 72.4, 80.7, 124.3, 130.5, 139.7, 141.2, 193.3.

2.1.3. Synthesis of pyrazoline derivatives (**3a–f**)

To a stirred solution of **2a–f** (10 mmol), in acetic acid (10 mL) hydrazine monohydrate (1.25 mL, 25 mmol) was added and reaction mixture was heated to reflux for 3 h. The solvent was evaporated under reduced pressure and water (50 mL) was added to the colored residue. Products were extracted from the reaction mixture with toluene or toluene/EtOAc (95:5) mixture. After removal of the main part of solvent the residue was filtered over SiO_2 pad. After evaporation of solvent oily residue was dissolved in ether, from which some of products **3a–f** crystallize on standing in deepfreeze.

2.1.3.1. 1-(3-Ferrocenyl-4,5-dihydro-1H-pyrazol-1-yl)ethanone (3a). Light orange crystals; mp 184–185 °C; Yield 85%; IR (cm^{-1}): 3085, 1650 (CO), 1502 (C=Carom.), 1418, 1311, 1104, 1029, 1011; ^1H NMR: δ 2.33 (s, 3H), 3.06–3.15 (m, 2H), 3.91–4.01 (m, 2H), 4.18 (s, 5H), 4.39 (t, $J = 1.8$ Hz, 2H), 4.61 (t, $J = 2.0$ Hz, 2H); ^{13}C NMR: δ 21.4, 33.0, 43.3, 67.3, 69.4, 70.2, 75.4, 157.3, 168.5 (CO). ESI-MS (40 eV): m/z (%) = 296 (100%) [$\text{M}]^+$, 254 (35%), 185 (12%), 121 (39%), 43 (7%).

2.1.3.2. 1-(5-Methyl-3-ferrocenyl-4,5-dihydro-1H-pyrazol-1-yl)ethanone (3b). Red-orange oil; Yield 81.2%; IR (cm^{-1}): 3086, 1648 (CO), 1498, 1413, 1314, 1106, 1027, 1006; ^1H NMR: δ 1.38 (d, $J = 6.6$ Hz, 3H), 2.31 (s, 3H), 2.65 (dd, $J = 17.2$, 3.4 Hz, 1H), 3.32 (dd, $J = 17.2$, 10.8 Hz, 1H), 4.19 (s, 5H), 4.39 (s, 2H), 4.57 (m, 1H), 4.63

(s, 2H); ^{13}C NMR: δ 20.3, 21.9, 41.6, 51.8, 67.2, 67.5, 69.4, 70.2, 75.7, 156.0, 168.3 (CO). ESI-MS (40 eV): m/z (%) = 310 (100%) [$\text{M}]^+$, 268 (31%), 185 (10%), 121 (27%), 43 (8%).

2.1.3.3. 1-(5,5-Dimethyl-3-ferrocenyl-4,5-dihydro-1H-pyrazol-1-yl)ethanone (3c). Cinnabar red crystals; mp 142 °C; Yield 61.2%; IR (cm^{-1}): 3086, 2929, 1651 (CO), 1498, 1405, 1314, 1105, 1012; NMR: δ ^1H NMR: δ 1.65 (s, 6H), 2.29 (s, 3H), 2.99 (s, 2H), 4.18 (s, 5H), 4.37 (t, $J = 1.8$ Hz, 2H), 4.57 (t, $J = 2.0$ Hz, 2H); ^{13}C NMR: δ 23.3, 26.3, 50.6, 62.8, 67.1, 69.3, 70.1, 72.3, 76.0, 153.6, 169.0 (CO). ESI-MS (40 eV): m/z (%) = 324 (100%) [$\text{M}]^+$, 283 (27%), 267 (63%), 185 (9%), 121 (27%), 43 (9%).

2.1.3.4. 1-(4-Methyl-3-ferrocenyl-4,5-dihydro-1H-pyrazol-1-yl)ethanone (3d). Cinnabar red crystals; mp 78–79 °C; Yield 81.2%; IR (cm^{-1}): 3099, 2974, 1655 (CO), 1496, 1449, 1308, 1160, 1106, 1028, 997; ^1H NMR: δ 1.14–1.85 (m, 2H), 1.71 (s, 3H), 2.33 (s, 3H), 3.29–3.45 (m, 1H), 4.18 (s, 5H), 4.41 (m, 2H), 4.59 (m, 1H), 4.69 (m, 1H); ^{13}C NMR: δ 19.8, 21.3, 40.5, 51.9, 67.4, 67.5, 69.6, 69.9, 70.2, 75.7, 161.4, 168.9 (CO). ESI-MS (40 eV): m/z (%) = 310 (100%) [$\text{M}]^+$, 268 (32%), 185 (19%), 121 (33%), 44 (30%).

2.1.3.5. (E)-1-(3-Ferrocenyl-5-propenyl-4,5-dihydro-1H-pyrazol-1-yl)ethanone (3e). Red-orange oil; Yield 78.4%; IR (cm^{-1}): 3086, 1654 (CO), 1497, 1412, 1378, 1106, 1007; ^1H NMR: δ 1.71 (dt, $J = 6.4$, 1.3 Hz, 3H), 2.82 (dd, $J = 17.0$, 3.8 Hz, 1H), 3.32 (dd, $J = 17.2$, 11.2 Hz, 1H), 4.12 (s, 5H), 4.39 (m, 2H), 4.54 (dt, $J = 3.8$, 1.6 Hz, 1H), 4.66 (dt, $J = 3.8$, 1.8 Hz, 1H), 5.01 (ddd, $J = 10.3$, 5.6, 4.0 Hz, 1H), 5.48 (ddd, $J = 15.2$, 6.0, 1.0 Hz, 1H), 5.69 (ddd, $J = 15.2$, 6.1, 1.0 Hz, 1H); ^{13}C NMR: δ 21.8, 43.7, 55.9, 58.9, 67.1, 67.6, 69.3, 70.2, 70.4, 75.4, 108.9, 111.6, 117.2, 134.7, 148.4, 149.3, 155.8, 168.2 (CO). ESI-MS (40 eV): m/z (%) = 336 (100%) [$\text{M}]^+$, 294 (17%), 185 (6%), 121 (21%), 43 (7%).

2.1.3.6. 1-(5-(Furan-2-yl)-3-ferrocenyl-4,5-dihydro-1H-pyrazol-1-yl)ethanone (3f). Cinnabar red crystals; mp 153 °C; Yield 59.5%; IR (cm^{-1}): 3101, 1651 (CO), 1498, 1416, 1376, 1309, 1149, 1156, 1018, 1006; ^1H NMR: δ 2.32 (s, 3H), 3.39 (m, $J = 17.2$, 11 Hz, 2H), 4.21 (s, 5H), 4.41 (m, 2H), 4.51 (m, 1H), 4.75 (m, 1H), 5.63 (m, $J = 11$, 0.23 Hz, 1H), 6.35 (s, 2H), 7.34 (s, 1H); ^{13}C NMR: δ 21.8, 39.3, 52.6, 66.8, 67.9, 69.5, 70.2, 70.5, 75.2, 107.5, 110.6, 141.7, 156.1, 168.2 (CO). ESI-MS (40 eV): m/z (%) = 362 (100%) [$\text{M}-16]^+$, 320 (29%), 185 (4%), 121 (21%), 43 (10%).

2.2. Antimicrobial activity

Antimicrobial activities of tested compounds were evaluated against five strains of bacteria: *Staphylococcus aureus* (ATCC 25923), *Bacillus subtilis* (ATCC 6633), *B. cereus* (ATCC 10987), *Escherichia coli* (ATCC 25922) and *Proteus mirabilis* (ATCC 29906) and seven species of fungi: *Aspergillus flavus* (ATCC 9170), *A. fumigatus* (ATCC 1022), *Candida albicans* (ATCC 10259), *Penicillium italicum* (ATCC 10454) and *Trichophyton mentagrophytes* (ATCC 9533), *Geotrichum candidum* (ATCC 34614) and *Mucor mucedo* (ATCC 20094) obtained from the American Type Culture Collection (ATCC).

The bacteria isolates were picked from overnight cultures in Mueller-Hinton agar and suspensions were prepared in sterile distilled water. The turbidity of suspensions was adjusted by comparing with 0.5 McFarland's standard to approximately 10^8 CFU/mL.

Fungal suspensions were prepared from 3- to 7-day-old cultures that grew on a potato dextrose agar except for *C. albicans* that was maintained on Sabouraud dextrose (SD) agar. The spores were rinsed with sterile distilled water, used to determine turbidity spectrophotometrically at 530 nm NCCLS [28]. The resulting suspensions were approximately 10^6 CFU/mL.

The 96-well microtiter assay using resazurin as the indicator of cell growth [29,30], was employed for the determination of the minimum inhibitory concentration (MIC) of the active components. Starting solutions of tested compounds were obtained by dissolving it in 5% DMSO. Next, serial twofold dilutions of tested compounds were made in a concentration range from 10 to 0.004 mg/mL in sterile 96-well plates containing Mueller-Hinton broth for bacterial cultures and a SD broth for fungal cultures. After that, diluted bacterial and fungal suspensions were added to appropriate wells and finally, resazurin solution was added as an indicator to each well. The inoculated plates were incubated at 37 °C for 24 h for bacteria and 28 °C for 72 h for fungi. The MIC was determined visually and defined as the lowest concentration of tested compounds that prevented resazurin color change from blue to pink. Streptomycin and ketoconazole were used as a positive control. Solvent control test was performed to study an effect of 5% DMSO on the growth of microorganism.

2.3. X-ray crystallography

Single-crystal X-ray diffraction data for compounds **2c**, **3c** and **3f** were collected on an Oxford Gemini S diffractometer equipped with a CCD detector, using monochromatized Mo K α radiation ($\lambda = 0.71073$ Å). Data reduction and empirical absorption correction were performed with CrysAlisPRO [31]. The structures were solved by direct methods using SHELXS and refined on R^2 by full-matrix least-squares using SHELXL [32]. All non-H atoms were refined anisotropically. H atoms were placed at geometrically calculated positions with the C–H distances fixed to 0.93 from Csp² and 0.98, 0.97 and 0.96 Å from methine, methylene and methyl Csp³, respectively. The corresponding isotropic displacement parameters of the H atoms were equal to 1.2 U_{eq} and 1.5 U_{eq} of the parent Csp² and Csp³, respectively. In compound **3c** the substituted cyclopentadienyl ring was found disordered over two sites with occupancies of 0.59(2) and 0.41(2), also in compound **3f** the unsubstituted cyclopentadienyl ring in the crystallographically independent molecule B was found disordered over two sites with occupancies of 0.56(2) and 0.44(2). In both compounds the disordered rings were modeled by AFIX 56, while the thermal parameters of the corresponding carbon atoms were restrained by SIMU instruction from the SHELXL [32]. Crystallographic details for structure analysis of compounds **2c**, **3c** and **3f** are summarized in Table 1. The crystal structures of compounds including the atom labeling schemes are presented in Fig. 1, while selected geometrical parameters are listed in Tables 3 and 4. Compound **3f** crystallizes with two crystallographically independent molecules in the asymmetric unit. There is no symmetry relation between two independent molecules (Fig. 1c). Figures were produced using ORTEP-3 [33] and MERCURY [34]. The software used for the preparation of the materials for publication: WINGX [35], PLATON [36], PARST [37].

3. Results and discussion

3.1. Synthesis

As mentioned in the Introduction section, we prepared, starting from conjugated ferrocenyl ketones **2a–f**, a series of ferrocenyl pyrazoline derivatives **3a–f** following the literature procedure [38], and tested their microbial activity.

Ferrocene **1** was acylated *in situ* with prepared acyl chlorides under Friedel-Crafts conditions yielding corresponding acyl-ferrocenes **2a–e** on which enone system is presented. Compounds **2a–d** were earlier described [39–43] whereas **2e** is a new compound, Scheme 1, and their spectral data are given. The main reason why chalcone **2f** was included in the experiments is fact that

Table 1
Crystallographic data for the crystal structures of **2c**, **3c** and **3f**.

	C ₁₅ H ₁₆ FeO	C ₁₇ H ₂₀ FeN ₂ O	C ₁₉ H ₁₈ FeN ₂ O ₂
Empirical formula	C ₁₅ H ₁₆ FeO	C ₁₇ H ₂₀ FeN ₂ O	C ₁₉ H ₁₈ FeN ₂ O ₂
Formula weight	268.13	324.20	362.20
Colour, crystal shape	Orange, prism	Orange, prism	Orange, prism
Crystal size (mm ³)	0.19 × 0.20 × 0.41	0.45 × 0.54 × 0.61	0.20 × 0.28 × 0.45
Temperature (K)	293(2)	293(2)	293(2)
Wavelength (Å)	0.71073	0.71073	0.71073
Crystal system	Monoclinic	Monoclinic	Triclinic
Space group	<i>P</i> 2 ₁ / <i>c</i>	<i>P</i> 2 ₁ / <i>n</i>	<i>P</i> 1–
Unit cell dimensions			
<i>a</i> (Å)	7.4494(3)	10.1531(5)	10.6668(4)
<i>b</i> (Å)	16.2301(7)	15.5466(7)	10.9147(4)
<i>c</i> (Å)	10.6694(5)	10.8705(5)	15.2710(6)
α (°)	90	90	109.838(4)
β (°)	96.858(3)	112.631(6)	100.165(3)
γ (°)	90	90	94.941(3)
<i>V</i> (Å ³)	1280.7(1)	1583.8(2)	1625.6(1)
<i>Z</i>	4	4	4
<i>D</i> _{calc} (Mg/m ³)	1.391	1.360	1.480
μ (mm ⁻¹)	1.157	0.952	0.941
θ range for data collection (°)	2.51–29.06	2.62–29.06	2.58–29.07
Reflections collected	7073	14,032	28,480
Independent reflections, <i>R</i> _{int}	2954, 0.0215	3773, 0.0214	7740, 0.0281
Data/restraints/parameters	2954/0/160	3773/36/221	7740/36/463
Goodness-of-fit	1.115	1.014	1.047
Final <i>R</i> ₁ / <i>wR</i> ₂ indices [<i>I</i> > 2 σ (<i>I</i>)]	0.0382/ 0.0861	0.0365/ 0.0865	0.0390/ 0.0948
Final <i>R</i> ₁ / <i>wR</i> ₂ indices (all data)	0.0530/ 0.0938	0.0505/ 0.0940	0.0519/ 0.1020
Largest diff. peak and hole (e Å ⁻³)	0.223/–0.453	0.269/–0.215	0.440/–0.320

heterocyclic ring is more reactive and polarized (heteroatom close to the conjugated double bonds) than common aromatic ring, and we suppose that will have different activity from chalcone like compounds.

Synthesized enone compounds **2a–f** (acyl-ferrocenes) reacts with hydrazine in boiling acetic acid [38], forming new, crystalline pyrazoline derivatives **3a–f**, Scheme 2.

3.2. Spectral characterization

All synthesized compounds were characterized by IR, ¹H and ¹³C NMR spectral data. In IR spectra of the synthesized compounds the most recognizable band appears in the carbonyl group region 1661–1648 cm⁻¹ (CH₃CO–).

In ¹H NMR spectra of compounds **3a–f** could be recognized characteristic signals corresponding to the 4H- and 5H-protons of pyrazoline ring. Those protons appear at 2.65–4.57 region, as singlet (2.99, 2H, compound **3c**), multiplet (3.06–3.15 or 3.91–4.01, 2H, compound **3a**) or doublet of doublet (2.65, 1H, compound **3c**, 2.82, 1H compound **3e**). Position and structure of signals are dependent on presence of substituents at 4- and 5-position of pyrazoline ring.

3.3. Antimicrobial activity

Antimicrobial activity of compounds **3a–f** were tested against 12 strains of microorganisms, including the agents of human, animal and plant diseases, mycotoxin producers, and food spoilage agents. The results of *in vitro* testing of antibacterial and antifungal activities of tested compounds in relation to selected species of microorganisms are shown in Table 2. The MIC values are the same in several cases because a series of double dilutions of the tested

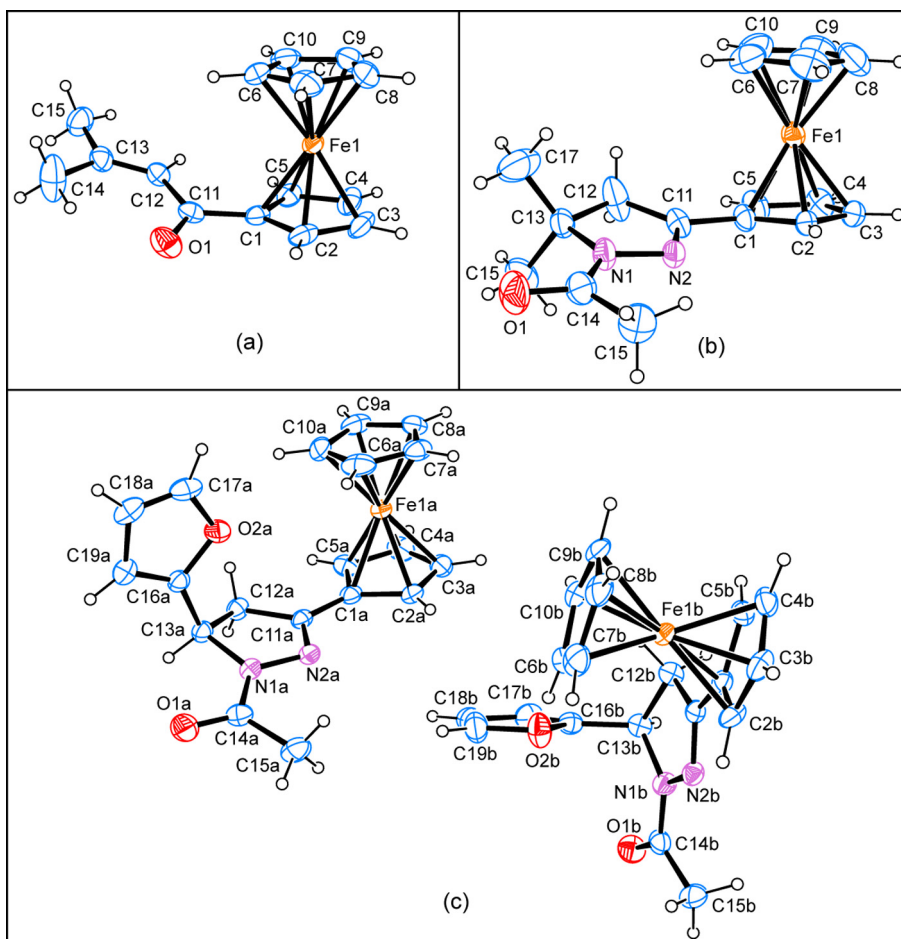


Fig. 1. The molecular structure of: (a) **2c**, (b) **3c** and (c) **3f** with the atom-labeling scheme. Only the major component of molecules **3c** and **3f** is presented (see Figs. S2 and S4, for disordered **3c** and **3f**, respectively). Displacement ellipsoids are drawn at the 30% probability level.

Table 2

Antibacterial and antifungal activity of compounds **3a–f**, minimum inhibitory concentration (MIC).

Compound	Microorganisms											
	<i>Staphylococcus aureus</i>	<i>Bacillus subtilis</i>	<i>Bacillus cereus</i>	<i>Escherichia coli</i>	<i>Proteus mirabilis</i>	<i>Aspergillus flavus</i>	<i>Aspergillus fumigatus</i>	<i>Candida albicans</i>	<i>Penicillium italicum</i>	<i>Trichophyton mentagrophytes</i>	<i>Geotrichum candidum</i>	<i>Mucor mucedo</i>
3a	0.312	0.156	0.078	0.625	0.312	2.5	2.5	1.25	2.5	1.25	1.25	2.5
3b	0.156	0.039	0.039	0.156	0.156	0.312	0.312	0.312	0.312	0.312	0.156	0.312
3c	0.312	0.078	0.078	0.312	0.312	2.5	0.625	0.625	1.25	0.625	0.625	0.625
3d	0.312	0.078	0.078	0.312	0.312	1.25	0.625	0.625	0.625	0.312	0.625	1.25
3e	0.078	0.039	0.039	0.156	0.156	0.312	0.312	0.156	0.312	0.156	0.312	0.156
3f	0.625	0.156	0.156	1.25	1.25	2.5	1.25	0.625	1.25	1.25	0.625	1.25
Antibiotics	0.031	0.016	0.016	0.062	0.062	0.156	0.156	0.039	0.156	0.078	0.078	0.156

Values given as mg/mL.

Antibiotics: Streptomycin (for bacteria) and Ketoconazole (for fungi).

compounds was used in the experiment against every tested microorganism.

Regarding the tested bacteria, the MIC for tested compounds ranged from 0.039 to 2.5 mg/mL. The most sensitive bacteria were *B. subtilis* and *B. cereus* with MIC values between 0.039 and 0.312 mg/mL. Moderate activity was shown against *S. aureus* with MIC at 0.078–1.25 mg/mL, while the highest resistance was shown in *P. mirabilis* and *E. coli*.

Antifungal activity was a slightly weaker than antibacterial. The MIC for tested compounds relative to the fungi ranged from 0.156 to 5 mg/mL. *C. albicans* and *T. mentagrophytes* appeared to be the most sensitive fungi (MIC values were from 0.156 to 1.25 mg/mL).

The other tested fungi have shown sensitivity at the higher concentrations (MIC ranged from 0.312 to 5 mg/mL). Solvent control showed that 5% DMSO had no inhibitory effect on the tested microorganisms.

Among tested compounds, **3e** showed marked inhibitory activity of the growth of selected bacteria and fungi in low concentrations. This compound can be a new, potential antimicrobial agent since these selected tested microorganisms have been developing resistance to common antibiotics.

In this study, the noticeable results were that the tested compounds inhibited the growth of Gram-negative bacteria and fungi at the highest tested concentrations than Gram-positive bacteria.

Table 3
Selected bond lengths (Å) and bond angles (°) in crystal structures of **3c** and **3f**.

	3c	3f	
		A	B
N1–N2	1.386(2)	1.400(3)	1.392(3)
N1–C13	1.492(3)	1.484(3)	1.481(3)
N1–C14	1.346(3)	1.352(3)	1.347(3)
N2–C11	1.286(3)	1.286(3)	1.285(3)
O1–C14	1.232(3)	1.222(3)	1.222(3)
C11–C12	1.485(3)	1.505(3)	1.505(3)
C12–C13	1.532(3)	1.529(3)	1.543(3)
C14–C15	1.494(3)	1.498(4)	1.499(4)
N1–N2–C11	108.1(2)	107.4(2)	107.8(2)
N1–C13–C12	100.8(2)	100.5(2)	100.6(2)
N1–C14–O1	120.7(2)	120.0(2)	120.8(2)
N2–N1–C13	112.8(2)	112.3(2)	112.9(2)
N2–C11–C12	114.4(2)	114.0(2)	114.1(2)
C11–C12–C13	103.5(2)	102.2(2)	102.3(2)

These results are not unexpected, considering that is known that Gram-negative bacteria, in contrast to Gram-positive bacteria, contain the outer membrane which serves as a permeability barrier and prevent the entry of noxious compounds including antibacterial compounds. The cell walls of fungi are the least permeable and consist of polysaccharides such as chitin and glucan, and it is the reason for their greater resistance [29,30,28].

The experimental results of antimicrobial activity of tested compounds may open the possibility of their potentially use in medicine, food production and pharmaceutical industry.

3.4. Description of crystal structures **2c**, **3c** and **3f**

In the precursor compound **2c** (Fig. 1a) the cyclopentadienyl (Cp) rings of the ferrocene unit (Fc) adopt nearly eclipsed geometry, with the C1–Cg1–Cg2–C6 torsion angle of 3.2° (Cg1 and Cg2 are centroids of the substituted and unsubstituted Cp rings, respectively). The Cp rings show a slight mutual tilting as evidenced by a dihedral angle between their mean planes of 2.5(2)°. The Fe...Cg distances display typical features of the monosubstituted ferrocenes where the distance of the Fe atom towards centroid of the substituted Cp ring is somewhat shorter than a distance to the centroid of unsubstituted ring (1.639 and 1.652 Å, respectively). The aliphatic fragment attached to the Fc unit is essentially planar with the r.m.s. deviation of non-H atoms from the mean plane of 0.027 Å and the largest deviation of atom C11 [0.044(2) Å]. Besides the carbonyl C11–O1 [1.227(2) Å] the shortest bond involving

non-H atoms of **2c** molecule is C12–C13 bond of the aliphatic fragment [1.331(3) Å]. The bonds involving carbonyl C11 atom have similar lengths [C1–C11 1.468(3) and C11–C12 1.476(3) Å], both shorter than a single C–C bond length (1.54 Å [44]). The approximately planar aliphatic fragment noticeably deviates from the level of Cp ring forming the dihedral angle with the corresponding Cp mean plane of 23.0(2)°. While the carbonyl O1 alone deviates from the Cp plane for 0.093(4) Å [torsion angle C2–C1–C11–O1 = –19.8(3)°] the deviation gradually increases toward the terminal atoms resulting in maximal deviation for the methyl C15 [1.458(8) Å]. The carbonyl O1 as well as the terminal methyl groups of the aliphatic fragment plays a important role in intermolecular interactions, stabilizing the crystal structure of **2c**.

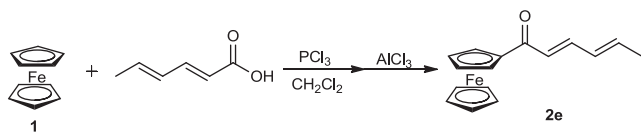
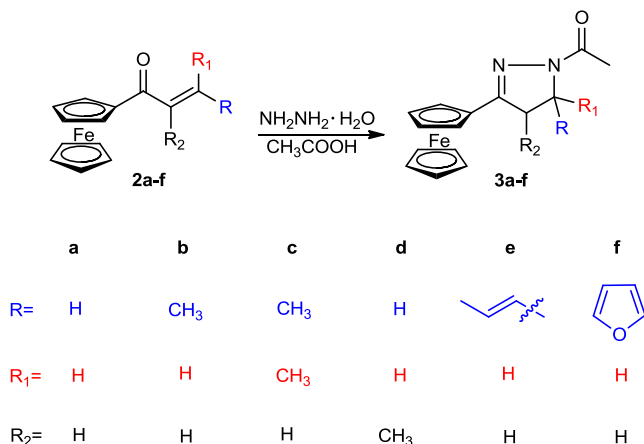
Due to the absence of polar hydrogen bonding donors, the crystal packing of **2c** is mainly stabilized by weak C–H...O and C–H...π interactions (Table 4). The bifurcated hydrogen bond C5–H5...O1 and C12–H12...O1 involving Cp and aliphatic C–H donors is the shortest intermolecular interaction which connects the molecules into a chain extending along the *c* crystallographic axis (Table 4, see also Supplementary material, Fig. S1a). Within the chain the Fc units of linked molecules have nearly orthogonal mutual orientation, so that the dihedral angle between the substituted Cp rings of the neighboring units equals to 87.2°. In this arrangement, each Cp ring of Fc units serves as π-acceptor of methyl donors in two weak interactions, C14–H14b...π and C15–H15b...π (Table 4, Fig. S1b). The 2D layers developed by these C–H...π interactions in *ab* plane interlink by C–H...O chains to form 3D crystal structure of **2c**.

The ferrocene-based compound **3c** (Fig. 1b) comprises the pyrazoline ring bonded to one Cp ring of the Fc unit. Selected bond distances and angles are summarized in Table 3.

The pyrazoline ring attached to the disordered Cp ring is fully ordered. The geometry of this ring is normal and closely comparable with those of previously reported Fc derivatives comprising the *N*-acetyl-pyrazoline substituent [45–47] The single C12–C13 bond [1.532(3) Å] is the longest bond of the pyrazoline ring, while the remaining bonds display intermediate lengths reflecting the existence of the π-electron delocalization over the ring system (Table 3). The r.m.s. deviation of the non-H atoms constituting the pyrazoline ring is 0.026 Å with the largest deviation from the mean plane observed for atom C13 [0.035(2) Å] leading to an envelope-like conformation. As expected, the acetyl group attached to N1 atom lies in the pyrazoline plane [dihedral angles between the planes is 1.5(3)°], while the oxygen atom takes *trans* position relative to pyrazoline N2 [torsion angle N2–N1–C14–O1

Table 4
Geometrical parameters for intermolecular C–H...O and C–H...π interactions in crystal structures of **2c**, **3c** and **3f** (Cg1, Cg2, Cg3 and Cg4 are centroids of the C1–C5, C6–C10, C16a–O2a and C16b–O2b ring, respectively).

D–H...A	D–H (Å)	H...A (Å)	D–H...A (°)	Symmetry codes:
2c				
C5–H5...O1	0.93	2.45	158	x, –y + 0.5, z – 0.5
C12–H12...O1	0.93	2.49	174	x, –y + 0.5, z – 0.5
C15–H15b...Cg1	0.96	3.20	151	x + 1, y, z
C14–H14b...Cg2	0.96	3.25	131	x, y + 0.5, –z + 1.5
3c				
C3–H3...O1	0.93	2.51	128	x, y, z + 1
C16–H16c...Cg1	0.96	3.15	121	–x, –y, –z + 1
3f				
C18a–H18a...O1a	0.93	2.50	166	–x, –y, –z + 1
C7b–H7b...O2b	0.93	2.51	163	–x + 1, y, z
C13a–H13a...O1b	0.98	2.55	133	–x + 1, –y + 1, –z + 1
C7a–H7a...Cg3	0.93	2.73	158	–x + 1, –y + 2, –z + 1
C10b–H10b...Cg3	0.93	2.72	157	x, y – 1, z
C19a–H19a...Cg4	0.93	2.83	144	x, y + 1, z
C12a–H12a...Cg4	0.98	3.21	134	–x + 1, –y + 1, –z + 1
C15a–H15b...Cg1a	0.96	3.10	144	–x + 1, –y, –z + 1

Scheme 1. Synthesis of ketone **2e**.Scheme 2. Reaction of ferrocenyl ketones **2** with hydrazine in AcOH.

176.4(2)°. Finally, the plane C13/C16/C17 containing the non-H atoms of methyl substituents is orthogonally positioned with respect to the pyrazoline ring (89.5(1)°). The torsion angle N2–C11–C1–C2 relating the substituent and adjacent Cp ring has the values of –20.1(7) and –6.7(10)° for major and minor component of the ring.

In the crystal packing of **3c** the acetyl O1 atom represents the most important H-bonding acceptor. The shortest C3–H3...O1 interaction actually involves the C–H donor from the disordered Cp ring, thus the geometry of this interaction differs for the major and minor component of Cp ring: H3...O1 2.51/2.33 Å and C3–H3...O1 126/155°. Though displaying more favorable parameters the minor component also implies the increased sterical interaction between the H atoms. The occurrence of such an interaction conflict might explain why this Cp ring is disordered between two positions. Nevertheless, the C3–H3...O1 is the leading intermolecular interaction which connects the molecules of **3c** into a chain extending along the *c* crystallographic axis (Fig. S3). The molecules from the neighboring chains are interconnected by pairs of centrosymmetric C16–H16c...π interactions where ordered Cp ring has the role of π acceptor for the methyl donor (Table 4).

The C–C and C–N distances in the pyrazoline rings of independent molecules (Table 3) closely agree with the values observed for **3c**. In comparison to **3c**, the pyrazoline rings in A and B show somewhat higher deviation of the constituting atoms from the corresponding mean planes (r.m.s deviation of 0.083 and 0.067 in A and B, respectively), with the largest deviation observed for C13 atom attaching the furyl ring [–0.112(2) and –0.090(2) for C13a and C13b, respectively]. The C2–C1–C11–N2 torsion angle of –12.3(3) and –18.3(3)° in A and B, respectively, shows that in both molecules the pyrazoline ring remains close to the level of substituted Cp ring. The overlay of independent molecules presented in Fig. 2 reveals difference in molecular conformation, which mainly concerns the different orientation of their furyl rings. This is reflected in N1–C13–C16–O2 torsion angle, which has the values of 74.6(2) and 54.2(3)° in A and B molecules, respectively. The angle between the least-squares planes of the furyl and the substituted Cp ring is 85.1(1) and 75.2(1)°, while the angle between planes of furyl and pyrazoline ring is 85.1(1) and 87.2(1)° in A

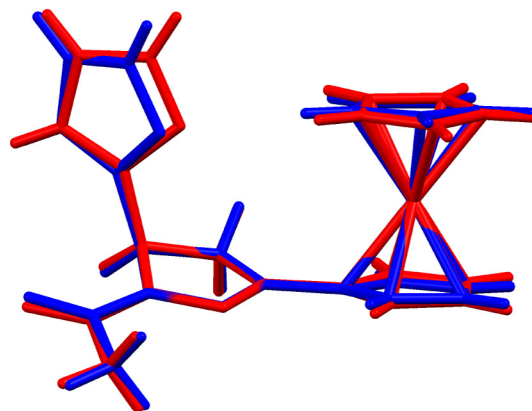


Fig. 2. Overlay of crystallographically independent molecules of **3f** based on a least-squares fit of atoms N1, N2 and C11 from the corresponding pyrazoline rings. The molecule shown in red is molecule A and that shown in blue is molecule B (major component). (For interpretation of the references to color in this figure legend, the reader is referred to the web version of this article.)

and B, respectively. The conformation of **3f** molecules is, as expected, markedly different from that of previously reported 3-(2-furyl)-5-ferrocenyl-2-pyrazoline isomer [47], where the Fc unit and furyl ring attach to sp³ and sp² C atoms of pyrazoline ring, respectively. In contrast to **3f**, such arrangement of molecular components leads to coplanarity between the pyrazoline and furyl rings (reported dihedral angle of 5.7(1), while 80.2° in average for **3f**) and orthogonal arrangement of pyrazoline and Cp ring [reported dihedral angle 81.4(1), while 17.0° in average for **3f**].

Crystal packing of **3f** is stabilized by a complex network of C–H...O and C–H...π interactions (Table 4). By means of C18a–H18a...O1a interaction formed between the furyl donor and carbonyl O1 acceptor the A molecules arrange into cyclic, centrosymmetric dimers (Fig. S5a). The molecules B do not display this type of dimer, instead there is a tendency of B molecules to form centrosymmetric dimer by C7b–H7b...O2b interaction involving the donor from disordered Cp ring and furyl oxygen as an acceptor. Unlike the carbonyl acceptor O1a, the acceptor O1b is employed in C13–H13a...O1b interaction (Table 4) that links the A and B dimers into a corresponding chain of dimers (Fig. S5a). The furyl rings from both independent molecules serve as π acceptors in four dissimilar C–H...π interactions (Table 4) which interconnect the chains of dimers toward 3D crystal structure (Fig. S5b).

4. Conclusion

We described herein synthesis, spectral, analytical, biological activity of series of compounds **3a–f**, and single crystal X-ray characterization of **2c** (starting ketone) and pyrazoline products **3c** and **3f** with ferrocene core. Synthesized compounds show significant antimicrobial activity, very close to streptomycin and ketoconazole (compound **3e** have equal activity as ketoconazole on *Mucor mucedo* fungi). From the experimental results, we suppose that substituent at position 5- in pyrazoline ring is responsible for elevated activity.

X-ray structural analysis has shown that the Fc-pyrazoline fragment of the novel **3c** and **3f** compounds exhibits similar conformational properties. In both compounds the incorporated pyrazoline ring is characterized by an envelope-like conformation with the somewhat increased puckering in **3f**. The crystal packing of **3c** and **3f** molecules are both stabilized by weak C–H...O and C–H...π interactions, nevertheless the different additional substituents at the pyrazoline ring (dimethyl and furyl in **3c** and **3f**, respectively) significantly influence the manner of molecular interaction with the crystalline surrounding.

Acknowledgement

This work was supported by the Ministry of Science and Technological Development of the Republic of Serbia, Projects No. 172034 and 172014.

Appendix A. Supplementary data

The supplementary Crystallographic data for the structural analysis have been deposited with Cambridge Crystallographic Data Centre: Deposition number CCDC 1567081, 1567082 and 1567083 for compounds **2c**, **3c** and **3f** respectively. These data can be obtained free of charge via www.ccdc.cam.ac.uk/data_request/cif or from the Cambridge Crystallographic Data Centre, 12, Union Road, Cambridge, CB2 1EZ, UK; Fax: +44 1223 336033; e-mail: deposit@ccdc.cam.ac.uk.

Supplementary data associated with this article can be found, in the online version, at <https://doi.org/10.1016/j.ica.2017.11.061>.

References

- [1] V. Opletalova, *Cesk. Slov. Farm.* 49 (2000) 278–284.
- [2] N. Yayli, O. Ucuncu, A. Yasar, M. Kucuk, E. Akyuz, S.A. Karaoglu, *Turk. J. Chem.* 30 (2006) 505–514.
- [3] A.R. Trivedi, D.K. Dodiya, N.R. Ravat, V.H. Shah, *ARKIVOC XI* (2008) 131–141.
- [4] P.M. Sivakumar, S. Ganesan, P. Veluchamy, M. Doble, *Chem. Biol. Drug Des.* 76 (2010) 407–411.
- [5] S. Bag, S. Ramar, M.S. Degani, *Med. Chem. Res.* 18 (2009) 309–316.
- [6] K.L. Lahtchev, D.I. Batovska, S.P. Parushev, V.M. Ubiyovok, A.A. Sibirny, *Eur. J. Med. Chem.* 43 (2008) 2220–2228.
- [7] R.F. Vasilev, V.D. Kancheva, G.F. Fedorova, D.I. Batovska, A.V. Trofimov, *Med. Chem. Res.* 51 (2010) 507–515.
- [8] P.M. Sivakumar, P.K. Prabhakar, M. Doble, *Med. Chem. Res.* 19 (2010) 1–17.
- [9] S. Vogel, S. Ohmayer, G. Brunner, J. Heilmann, *Bioorg. Med. Chem.* 15 (2008) 4286–4293.
- [10] S. Mostahar, P. Katun, A. Islam, *J. Biol. Sci.* 7 (2007) 514–519.
- [11] L.F. Motta, A.C. Gaudio, Y. Takahata, *Int. Electron. J. Mol. Des.* 5 (2006) 555–569.
- [12] S.K. Awasthi, N. Mishra, B. Kumar, M. Sharma, A. Bhattacharya, L.C. Mishra, V.K. Bhasin, *Med. Chem. Res.* 18 (2009) 407–420.
- [13] X. Wu, P. Wilairat, M.N. Go, *Bioorg. Med. Chem. Lett.* 12 (2002) 2299–2302.
- [14] H.L. Yadav, P. Gupta, P.S. Pawar, P.K. Singour, U.K. Patil, *Med. Chem. Res.* 19 (2010) 1–8.
- [15] Z. Nowakowska, *Eur. J. Med. Chem.* 42 (2007) 125–137.
- [16] G. Achanta, A. Modzelewska, L. Feng, S.R. Khan, P. Huang, *Mol. Pharmacol.* 70 (2006) 426–433.
- [17] D. Kumar, N.M. Kumar, K. Akamatsu, E. Kusaka, H. Harada, T. Ito, *Bioorg. Med. Chem. Lett.* 20 (2011) 3916–3919.
- [18] W.D. Seo, Y.B. Ryu, M.J. Curtis-Long, C.W. Lee, H.W. Ryu, K.C. Jang, *Eur. J. Med. Chem.* 45 (2010) 2010–2017.
- [19] C. Echeverria, J.F. Santibanez, O. Donoso-Tauda, C.A. Escobar, R.R. Tagle, *Int. J. Mol. Sci.* 10 (2009) 221–231.
- [20] R. Romagnoli, P.G. Baraldi, M.D. Carrion, C.L. Cara, O. Cruz-Lopez, D. Preti, *Bioorg. Med. Chem.* 16 (2008) 5367–5376.
- [21] K. Ilango, P. Valentina, G. Saluja, *Res. J. Pharm. Biol. Chem. Sci.* 1 (2010) 354–359.
- [22] R. Kalirajan, S.U. Sivakumar, S. Jubie, B. Gowramma, B. Suresh, *Int. J. ChemTech. Res.* 1 (2009) 27–34.
- [23] L. Varga, T. Nagy, I. Kövesdi, J. Benet-Bucholz, G. Dorman, L. Úrge, F. Darvas, *Tetrahedron* 59 (2003) 655–662.
- [24] I. Damljanović, M. Vukičević, N. Radulović, R. Palić, E. Ellmerer, Z. Ratković, M. Joksović, R.D. Vukičević, *Bioorg. Med. Chem. Lett.* 19 (2009) 1093–1096.
- [25] Z. Ratković, Z.D. Juranić, T. Stanojković, D. Manojlović, R.D. Vukičević, N. Radulović, M.D. Joksović, *Bioorg. Chem.* 38 (2010) 26–32.
- [26] J. Muškinja, A. Burmudžija, Z. Ratković, B. Ranković, M. Kosanić, G.A. Bogdanović, S.B. Novaković, *Med. Chem. Res.* 25 (2016) 1744–1753.
- [27] A. Burmudžija, J. Muškinja, Z. Ratković, N. Janković, B. Ranković, M. Kosanić, S. Đorđević, *RSC Adv.* 6 (2016) 91420–91430.
- [28] NCCLS (National Committee for Clinical Laboratory Standards), NCCLS, Wayne, PA, USA (1998).
- [29] S.D. Sarker, L. Nahar, Y. Kumarasamy, *Methods* 42 (2007) 321–324.
- [30] Z. Ratković, J. Muškinja, A. Burmudžija, B. Ranković, M. Kosanić, G.A. Bogdanović, B. Simović-Marković, A. Nikolić, N. Arsenijević, S. Đorđević, R.D. Vukičević, *J. Mol. Struct.* 1109 (2016) 82–88.
- [31] Agilent, CrysAlis PRO, Agilent Technologies, Yarnton, Oxfordshire, England, 2013.
- [32] G.M. Sheldrick, *Acta Crystallogr. Sect. A* 64 (2008) 112–122.
- [33] L.J. Farrugia, *J. Appl. Crystallogr.* 30 (1997) 565.
- [34] C.F. Macrae, P.R. Edgington, P. McCabe, E. Pidcock, G.P. Shields, R. Taylor, M. Towler, J. van de Streek, *J. Appl. Crystallogr.* 39 (2006) 453–457.
- [35] L.J. Farrugia, *J. Appl. Crystallogr.* 32 (1999) 837–838.
- [36] A.L. Spek, *J. Appl. Crystallogr.* 36 (2003) 7–13.
- [37] M. Nardelli, *J. Appl. Crystallogr.* 28 (1995) 659.
- [38] A. Levai, J. Jakob, *ARKIVOC x* (2005) 199–205.
- [39] J. Tirouflet, J. Boichard, C. R. Acad. Sci. 250 (1960) 1861–1865.
- [40] V.K. Skubin, V.P. Redko, D.F. Kutepov, V.V. Korshak, *Vysokomol. Soedin.* 3 (1980) 222–224.
- [41] J. Tirouflet, B. Gautheron, R. Dabard, *Bull. Soc. Chim. France* 1 (1965) 96–102.
- [42] W.M. Horspool, R.G. Sutherland, B.J. Thomson, *J. Chem. Soc., Sect. C: Org.* 8 (1971) 1558–1563.
- [43] A.M. El-Khawaga, K.M. Hassan, A.A. Khalaf, *Z. Naturforsch.* 36B (1) (1981) 119–122.
- [44] F.H. Allen, O. Kennard, D.G. Watson, L. Brammer, A.G. Orpen, R. Taylor, *J. Chem. Soc., Perkin Trans.* 2 (1987) S1–S19.
- [45] V.G. Andrianov, Y.T. Struchkov, V.N. Postnov, E.I. Klimova, V.A. Sazonova, *J. Organomet. Chem.* 272 (1984) 81–89.
- [46] G.T. Cin, S. Demirel, N. Karadayi, O. Buyukgungor, *Acta Crystallogr., Sect. E* 64 (2008) m514–m515.
- [47] G.T. Cin, S.D. Topel, A. Cakici, A.O. Yildirim, A. Karadag, *J. Chem. Crystallogr.* 42 (2012) 372–380.